Exact enumeration results for self-avoiding walks on the honeycomb lattice attached to a surface

1996 J. Phys. A: Math. Gen. 29 4755

(http://iopscience.iop.org/0305-4470/29/16/004)

J. Phys. A: Math. Gen. **29** (1996) 4755–4768. Printed in the UK

Exact enumeration results for self-avoiding walks on the honeycomb lattice attached to a surface

D Bennett-Wood and A L Owczarek†

Department of Mathematics, The University of Melbourne, Parkville, Victoria 3052, Australia

Received 27 November 1995, in final form 29 February 1996

Abstract. We consider self-avoiding walks on the honeycomb lattice interacting with a surface with different energies associated between sites in contact with a linear boundary to the left of the origin and those in contact with the right of the boundary. We numerically confirm recent exact results for the polymer adsorption transition and corresponding critical exponents with mixed ordinary and special boundary conditions. The phase diagram is elucidated with the aid of some rigorous arguments.

1. Introduction

Long, flexible polymers in a good solvent have been studied extensively over many years in the context of critical phenomena, with a wide range of exact results found, particularly in two dimensions. A natural extension of this theory is to consider the effects of introducing an impenetrable wall into the solvent with one or both ends of the polymer being attached, and the rest restricted to an area above or below this surface. This wall can be thought of as an interface between a solid and a liquid.

The canonical model of polymers in a solvent is that of self-avoiding walks (SAW) on some lattice. The wall can be introduced by restricting the SAW to the upper half of a d-dimensional lattice and the interaction with the surface by an energy, $-\varepsilon$, associated with contacts between the polymer and the surface. The Boltzmann weight for a configuration of the polymer is given by $\kappa^m = \mathrm{e}^{m\varepsilon/k_\mathrm{B}T}$, where T is the temperature of the solvent and m is the number of contacts with the surface. At some critical temperature, T_a, the polymer becomes adsorbed onto the surface [1]. In a seminal paper in this field, Hammersley *et al* [1] proved that there must be a phase transition in this model (on the hypercubic lattice). Given there is a single transition, it can be further shown [2] that at this adsorption transition the d-dimensional behaviour of the polymer becomes $(d-1)$-dimensional. For high temperatures, $(T > T_a)$, the polymer is in a desorbed phase where it extends a large distance into the solvent above the surface to which it is attached. For low temperatures, $(T < T_a)$, the polymer is in an adsorbed phase.

The adsorption of polymers has generated much interest, with many exact results found in two dimensions through conformal field theory [3–6] and using conformal invariance predictions in conjunction with the Bethe ansatz solution of associated lattice models [7–9]. In addition to this, much numerical work to find critical exponents has been completed in two dimensions using Monte Carlo [10, 11], exact enumeration [12–20], renormalization

† E-mail address: aleks@mundoe.maths.mu.oz.au

0305-4470/96/164755+14$19.50

group [21], transfer matrix [22, 23] and series expansions techniques [24] with varying degrees of success. Most of this work has been done on the square and triangular lattices.

It is well known [25] that there is a correspondence between SAW and the $O(n)$ model in the limit $n \to 0$. Burkhardt and Eisenriegler [6] considered the $O(n)$ model with three different boundary conditions: free boundary spins, where the bulk and surface couplings are the same; fixed boundary spins; and critically enhanced surface coupling. In the terminology of surface critical phenomena these three boundary conditions correspond to the 'ordinary', 'extraordinary' and 'special' transitions. The critical adsorption temperature, T_a, for SAW corresponds to the 'special' transition, and will be referred to as such throughout this paper. The 'ordinary' transition corresponds to SAW in the presence of an effectively repulsive surface.

Importantly, in a recent paper, Batchelor and Yung [8] derived the critical temperature and configurational exponent from the Bethe ansatz solution of the $O(n)$ loop model with mixed boundary conditions on the honeycomb lattice. Here, 'ordinary' (O) boundary conditions apply to one side of the walk's origin, and 'special' (S) boundary conditions apply to the other. Burkhardt and Eisenriegler [6] have also considered such mixed boundary conditions, calculating the universal Casimir contribution to the free energy via conformal invariance methods. Batchelor and Yung [8] also derived this quantity, along with the geometric scaling dimensions which describe the universal surface critical behaviour.

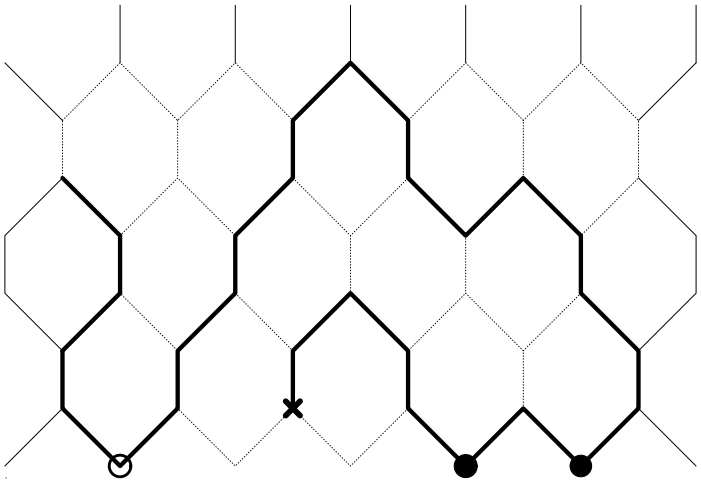

Figure 1. A self-avoiding walk on the honeycomb lattice attached to a one-dimensional boundary with contacts identified with the boundary to the left (open circles) and to the right (closed circles) of the origin (a cross). A fugacity κ_l is associated with open circle contacts while a fugacity κ_r is associated with closed circle contacts.

In this paper we consider SAW on the honeycomb lattice with fugacities κ_l and κ_r associated with contacts between the walk and either side of the surface as shown in figure 1. We have considered cases where both sides of the surface are 'special', both sides are 'ordinary', and the mixed case as explained above. In the cases of both sides of the surface being 'special', and both sides 'ordinary', we have been able to check exponent values that have been calculated previously on other lattices, and conjectured exactly on the honeycomb lattice where the connective constant and adsorption transitions are known exactly. We have

found† that in the case of both sides being 'ordinary', $\gamma_1^{(o)} = 0.953\,12 \pm 0.000\,52$, compared to the conjectured exact result [3] of $61/64 = 0.953\,125$. This numerical estimate is, in general, more accurate than those found in previous studies [14, 18, 17, 13, 15, 10] on the triangular and square lattices. For both sides being 'special', $\gamma_1^{(s)} = 1.450 \pm 0.004$, where here the conjectured exact result [7] is $93/64 = 1.453\,125$. Again, this numerical estimate is more accurate than those found in previous studies [16, 11, 10, 22] on the triangular and square lattices. The crossover exponent is also found to be $\phi_s = 0.520 \pm 0.013$, just outside the predicted [5] $\phi_s = \frac{1}{2}$. This estimate, however is no better or worse than all [11, 10, 21, 20] but a transfer matrix study [23] on the square lattice. We find also that $\phi_s^{(m)} = 0.514 \pm 0.014$, giving a numerical indication that $\phi_s^{(m)} = \frac{1}{2}$.

Importantly, we have been able to verify Batchelor and Yung's [8] new exponent conjecture $\gamma_1^{(m)} = 85/64 = 1.328\,125$, obtaining the value of $\gamma_1^{(m)} = 1.3279 \pm 0.0003$ for the mixed case as explained above. This has not been estimated previously.

Finally, we have been able to map out the complete phase diagram in the κ_l–κ_r plane. This has been accomplished by first modifying existing arguments [1] to prove the existence of the free energy. Bounds on its behaviour then enable us to delineate the phase boundaries and the order of the transitions across these boundaries. This is summarized in figure 2. One interesting feature is the first-order transition along the line $\kappa_l = \kappa_r$ for $\kappa_r \geqslant \kappa_a$.

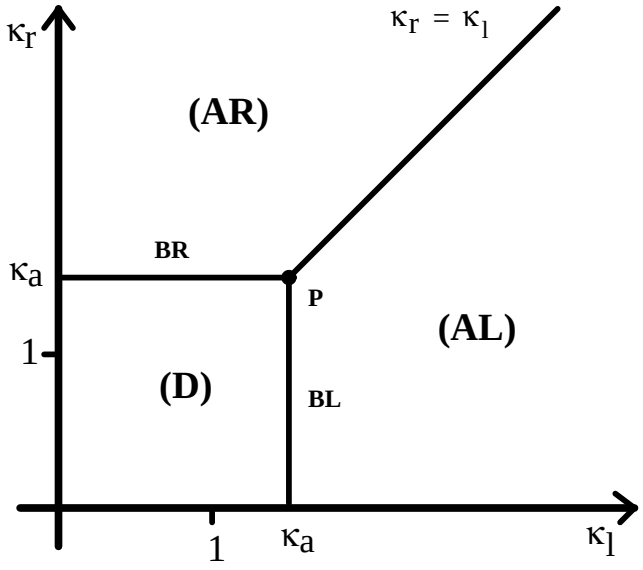

Figure 2. A schematic illustration of a conjectured phase diagram in the (κ_l, κ_r) plane showing the three phases: desorbed (D); adsorbed to the left side of the boundary (AL); and adsorbed to the right-hand side of the boundary (AR). This diagram also shows the phase boundaries BR and BL, and their point of intersection P. The transition (BR, BL, or P) from the desorbed phase into one of the others is critical while the transition from one adsorbed phase to the other should be first order.

This paper is set out as follows: the partition function and other quantities of interest are defined in section 2. We give a brief report on the generation of the walks and a discussion

† Note: for clarity we distinguish the configurational exponent for 'ordinary', 'special' and 'mixed' boundary conditions by the superscripts (o), (s) and (m), respectively.

of the techniques of analysis in section 3. Section 4 contains our best estimates of the various exponents. In section 5 we discuss the phase diagram and some brief conclusions follow in the final section.

2. The model

The partition function for walks of length n with one end attached to a surface, with different energies for sites interacting with either side of a surface is given by

$$Z_n^1(\kappa_l, \kappa_r) = \sum_{m_l, m_r} c_n(m_l, m_r)\kappa_l^{m_l}\kappa_r^{m_r} \tag{1}$$

where the sum is over all allowed values of the number of contacts m_l with the left-hand side of the surface, and the number of contacts m_r with the right. The coefficients $c_n(m_l, m_r)$ are the number of configurations of length n with m_l and m_r left- and right-hand interactions respectively. As described by figure 1, κ_l and κ_r are the respective fugacities of contacts to the left- and right-hand side of the surface. That is, κ_l and κ_r are given by $\kappa_l = \mathrm{e}^{\varepsilon_l/k_\mathrm{B}T}$ and $\kappa_r = \mathrm{e}^{\varepsilon_r/k_\mathrm{B}T}$ where $-\varepsilon_l$ and $-\varepsilon_r$ are the energies of a single contact with the left and right-hand side of the surface, respectively. While the average energy, given by $\langle E\rangle = -\langle \varepsilon_l m_l + \varepsilon_r m_r\rangle$, and the specific heat per step, given by $C_n(\kappa_l, \kappa_r) = \frac{\langle E^2\rangle - \langle E\rangle^2}{n}$, are canonical quantities to consider we have also found it advantageous to calculate the average number of contacts with each side $\langle m_l\rangle$ and $\langle m_r\rangle$ and their fluctuations,

$$F_n^l(\kappa_l, \kappa_r) = \frac{\langle m_l^2\rangle - \langle m_l\rangle^2}{n} \tag{2}$$

and

$$F_n^r(\kappa_l, \kappa_r) = \frac{\langle m_r^2\rangle - \langle m_r\rangle^2}{n} \tag{3}$$

separately.

The reduced free energy per step in the thermodynamic limit is

$$f(\kappa_l, \kappa_r) = \lim_{n\to\infty} \frac{1}{n} \ln Z_n^1(\kappa_l, \kappa_r). \tag{4}$$

Let us take $\kappa_l = \kappa_r$ for the moment. Then, it is known [1] (at least for the square lattice) that this limit

$$f(\kappa_r, \kappa_r) = \lim_{n\to\infty} \frac{1}{n} \ln Z_n^1(\kappa_r, \kappa_r) \tag{5}$$

exists. Moreover, for $0 \leqslant \kappa_l = \kappa_r \leqslant 1$

$$f(\kappa_r, \kappa_r) = \lim_{n\to\infty} \frac{1}{n} \ln Z_n^1(\kappa_r, \kappa_r) = \lim_{n\to\infty} \frac{1}{n} \ln Z_n = \ln \mu_{\mathrm{saw}} \tag{6}$$

where Z_n is the partition function for walks in the bulk. It has also been proved that

$$f(\kappa_r, \kappa_r) > \ln \mu_{\mathrm{saw}} \tag{7}$$

for sufficiently large κ_r. Hence there must be a least one non-analyticity in the function $f(\kappa_r, \kappa_r)$. Assuming that there is a single adsorption transition this then implies that there exists a value $\kappa_a > 1$ such that the result (6) holds for $0 \leqslant \kappa_l = \kappa_r \leqslant \kappa_a$.

In general, it is appropriate to assume that

$$Z_n^1 \sim A\,\mu^n n^{\gamma_1 - 1} \qquad \text{as } n \to \infty \tag{8}$$

and

$$Z_n \sim B\mu_{\rm saw}^n n^{\gamma-1} \qquad \text{as } n \to \infty \tag{9}$$

where A and B are constants, $\mu_{\rm saw}$ is the bulk connective constant, while $\mu = {\rm e}^{f(\kappa_l,\kappa_r)}$, and γ_1 and γ are the universal configurational exponents for walks with one end attached to the surface and walks in the bulk, respectively. In general, f and A vary continuously with temperature while the exponent γ_1 only changes if there is a change of phase. (Of course, if one only considers surface interactions the bulk partition function never changes!) However, in this problem the free energy f is also expected to be independent of temperature in the desorbed phase, and equal to the bulk value $\ln \mu_{\rm saw}$ as proved in the $\kappa_l = \kappa_r$ case mentioned above. (It is still expected to be lattice dependent.) Nienhuis [26] has found that $\mu_{\rm saw} = 1/x_{\rm c} = \sqrt{2+\sqrt{2}}$ for SAW on the honeycomb lattice.

Upon further consideration, to which we shall return in section 5, it can be argued that the free energy $f(\kappa_l, \kappa_r)$ exists for all $\kappa_l \geqslant 0$ and $\kappa_r \geqslant 0$, and has the following behaviour:

$$f(\kappa_l, \kappa_r) = \ln \mu_{\rm saw} \qquad \text{for } 0 \leqslant \kappa_l, \kappa_r \leqslant \kappa_a \tag{10}$$

while for any κ_l and κ_r

$$f(\kappa_l, \kappa_r) = f(\kappa_r, \kappa_r) \qquad \text{if } \kappa_l < \kappa_r \tag{11}$$

and

$$f(\kappa_l, \kappa_r) = f(\kappa_l, \kappa_l) \qquad \text{if } \kappa_l > \kappa_r. \tag{12}$$

This leads to the conjectured phase diagram illustrated in figure 2. We shall show in section 5 that this can indeed be proved (at least on the square lattice) with the help of results from Hammersley *et al* [1].

As mentioned in the introduction, we are particularly interested in the following three cases:

(i) (O–O): the entire surface is effectively repulsive. The value $\gamma_1^{(\rm o)} = 61/64$ has been conjectured using conformal field theory [3] and series results [17], and was later confirmed by Duplantier and Saleur [4].

(ii) (S–S): the entire surface is critically adsorbing. Batchelor and Yung [7] found that $\gamma_1^{(\rm s)} = 93/64$ by means of the Bethe ansatz. Guim and Burkhardt [22] conjectured this some years earlier, on the basis of conformal invariance arguments which follow from the work of Duplantier and Saleur [4].

(iii) (O–S): the surface is mixed, with one half repulsive and the other adsorbing. Batchelor and Yung [8] recently found that $\gamma_1^{(\rm m)} = 85/64$, again by means of the Bethe ansatz.

It is this third situation which is new and we have examined with a view to testing the predictions of Batchelor and Yung [8].

Batchelor and Yung [7] found that the critical temperature for adsorbing polymers on the honeycomb lattice is given by $\kappa_l = \kappa_r = 1 + \sqrt{2} \equiv \kappa_a$ in the symmetric interaction case. They then showed [8] that if one considers the line $\kappa_l = 1$ the adsorption point is $\kappa_l = 1, \kappa_r = \kappa_a$. Hence, this is a mixed boundary point (O–S) as described above. Note that this is consistent with the free energy behaviour also described above. These exact interaction values allow one to test exponent conjectures for all three boundary conditions described above, that is (O–O), (S–S) and (O–S).

It is also expected that at the special point the average number of contacts scales as

$$\langle m \rangle \sim n^{\phi_s} \tag{13}$$

where ϕ_s is known as the crossover exponent and

$$\langle m \rangle = \frac{\sum_{m_l,m_r} m c_n(m_l,m_r)\kappa_l^{m_l}\kappa_r^{m_r}}{\sum_{m_l,m_r} c_n(m_l,m_r)\kappa_l^{m_l}\kappa_r^{m_r}} \tag{14}$$

where $m = m_l + m_r$. Burkhardt *et al* [5] found using conformal invariance arguments that $\phi_s = \frac{1}{2}$. One can consider an analogous exponent for the (O–S) case: this crossover exponent $\phi_s^{(m)}$ is then defined by

$$\langle m_r \rangle \sim n^{\phi_s^{(m)}} \tag{15}$$

at $\kappa_l = 1$, $\kappa_r = \kappa_a$. Now, the behaviour mentioned above in equations (11) and (12), and discussed in section 5, can be used to argue, with some mild assumptions, that $\phi_s^{(m)} = \phi_s$. This can also be inferred from the calculation of Guim and Burkhardt [23] utilizing the associated conformal field theory [27, 28, 6].

3. Exact enumerations

3.1. Calculation of series

We have used a simple backtracking algorithm [29] to directly enumerate all self-avoiding walks on the two-dimensional honeycomb lattice whose origin is attached to a one-dimensional impenetrable boundary. The number of contacts with the boundary on either side of the origin were counted separately.

The CPU time required for this algorithm to count all walks of length n grows exponentially with n. However, the total CPU time was reduced through the use of a multiprocessor Intel Paragon. By exploiting symmetry, we find that there are 80 independent configurations of length 8. These can therefore be programmed into 80 nodes (processors) of the Paragon. Using the backtracking algorithm, each of these nodes can then enumerate all walks of lengths 9–48 from the initial configuration independently, with the final totals obtained by a global sum over processors on completion. This resulted in a speed up of approximately 64.5, i.e. a parallelization of about 82%.

Our algorithm counted the number of walks $c_n(m_l, m_r)$ with m_l and m_r contacts with the left- and right-hand sides of the surface, respectively. The three partition function series which we have analysed for the (O–O), (S–S) and (O–S) cases are given in table 1, while the full series for the coefficients may be obtained via e-mail on request.

3.2. Analysis

We utilized second-order differential approximants [30] of the generating function $G(x) = \sum_n Z_n^1 x^n$ using the series $Z_n^1(\kappa_l, \kappa_r)$ in order to determine the critical point $x_c(\kappa_l, \kappa_r) = 1/\mu(\kappa_l, \kappa_r)$ and corresponding exponent, $\gamma_1(\kappa_l, \kappa_r)$ for various values of κ_l and κ_r which correspond to the following three cases: (O–O), (S–S) and (O–S). The generating function $H(x) = \sum_n \langle m \rangle x^n$ of the series $\langle m \rangle(\kappa_l, \kappa_r)$ was also used to estimate the crossover exponent ϕ_s. Briefly, the available series coefficients of the partition function are fitted sequentially to linear, quadratic and higher-order recurrence relations of a specific form [30] which can then be solved, giving linear homogeneous differential equations with polynomial coefficients. The solution of these equations allows us to make an estimate of the critical point and its corresponding exponent.

Any approximant in which there is a singularity on the positive real axis closer to the origin, or is beyond but close to the physical singularity is considered defective and is

Table 1. The enumerations of SAW on the honeycomb lattice in the presence of a one-dimensional boundary are summed to give the series for the partition functions used to explore the (O–O), (S–S) and (O–S) boundary conditions for lengths $n = 1$ to 48.

1	3	.5828427314758301e+01	.3414213657379150e+01
2	4	.6828427314758301e+01	.4414213657379150e+01
3	8	.2048528194427490e+02	.1224264097213745e+02
4	14	.2931370925903320e+02	.1865685462951660e+02
5	28	.8076955413818359e+02	.4638477706909180e+02
6	46	.1140832633972168e+03	.6904163169860840e+02
7	90	.2921076517105102e+03	.1670538258552551e+03
8	160	.4443330516815186e+03	.2621665258407593e+03
9	308	.1090974761130413e+04	.6038305253982544e+03
10	540	.1654905794681112e+04	.9556244697570801e+03
11	1032	.3923565991349023e+04	.2154569788932800e+04
12	1846	.6143917540497583e+04	.3476745563507080e+04
13	3502	.1420503943252600e+05	.7662725759983063e+04
14	6272	.2240920087188419e+05	.1248604912090302e+05
15	11852	.5078426451904527e+05	.2710315744638443e+05
16	21364	.8124232322888561e+05	.4462086089229584e+05
17	40234	.1811545576625838e+06	.9557572777938843e+05
18	72694	.2923807201142188e+06	.1585449418573380e+06
19	136564	.6433517213855848e+06	.3359741174321174e+06
20	247498	.1046453096934826e+07	.5610759009304047e+06
21	464070	.2276803796285042e+07	.1178318144832611e+07
22	842546	.3730422499645987e+07	.1978945443247795e+07
23	1577280	.8039413464318852e+07	.4123805802336693e+07
24	2868922	.1324500003611797e+08	.6959779401179314e+07
25	5364030	.2830719038509496e+08	.1440727740175867e+08
26	9769366	.4689567764791824e+08	.2442023612823772e+08
27	18245976	.9950326139253240e+08	.5025662946832752e+08
28	33272104	.1655725563778450e+09	.8550812893919277e+08
29	62086194	.3490552761706884e+09	.1750756319280586e+09
30	113326264	.5833163652649582e+09	.2988918007788830e+09
31	211304042	.1222728994290704e+10	.6091759172874007e+09
32	386039204	.2050821145962415e+10	.1043163353813419e+10
33	719319094	.4276787852344742e+10	.2117401685571724e+10
34	1315132086	.7197874703447445e+10	.3635881912641722e+10
35	2449100566	.1494095175569448e+11	.7352833995839876e+10
36	4480726500	.2522305217566550e+11	.1265754443011045e+11
37	8339980334	.5213585846726704e+11	.2551162901638902e+11
38	15267286682	.8826528896415058e+11	.4401781296908662e+11
39	28404168780	.1817410960044507e+12	.8844814250017940e+11
40	52024731994	.3084876797248815e+12	.1529303474997905e+12
41	96751072342	.6329399908381325e+12	.3064336893174523e+12
42	177291764826	.1076949329894609e+13	.5308667761897037e+12
43	329592919094	.2202428852746105e+13	.1060981981021724e+13
44	604222603778	.3755837034229572e+13	.1841360871232400e+13
45	1122911304344	.7657752537278444e+13	.3671353563908310e+13
46	2059361267316	.1308614099062022e+14	.6382398205724697e+13
47	3826073982642	.2660651375522593e+14	.1269730180736382e+14
48	7019302474024	.4555583011181758e+14	.2210786747309802e+14

discarded in any further analysis. In our analysis any approximant within a factor of 1.3 of the physical singularity is taken to be defective. More precisely, any approximants with singularities in the complex plane found within a strip bounded by ± 0.05i and $[0, 1.3x_c]$,

where x_c is the estimate of the physical singularity's position, are considered defective. The non-defective approximants were then averaged, with the error given as two standard deviations. Due to the number of approximants from some analyses produced here we have consistently pooled the approximants obtained from using different numbers of coefficients. This overestimates the error in some cases but should provide conservative estimates in most cases.

In section 5 we have used the fluctuations of the number of left- and right-hand contacts with the surface per step, $F_n^l(\kappa_l, \kappa_r)$ and $F_n^r(\kappa_l, \kappa_r)$, respectively, to search for possible phase transitions. We initially considered simple plots of $F_n^l(\kappa_l, \kappa_r)$ against κ_l for fixed $\kappa_r = d_1$ and various values of d_1. The positions of the maxima of these fluctuations along lines in the (κ_l, κ_r) plane gives us an indication of the location of any phase transitions. The analogous procedure was completed on $F_n^r(\kappa_l, \kappa_r)$ at fixed $\kappa_l = d_2$ to gain a full two-dimensional representation of the model's behaviour.

4. Results

As mentioned in the introduction, many authors have estimated the critical exponents numerically for two-dimensional SAW with 'ordinary' and 'special' boundary conditions, with most of this work having been done on the square and triangular lattices. We will also calculate these exponents, merely as a check of the consistency of our method of analysis, along with calculating the exponents for 'mixed' boundary conditions.

4.1. The (O–O) model

From direct enumeration on the triangular lattice De'Bell and Essam [14] first estimated $\gamma_1^{(o)} = 0.956^{+0.014}_{-0.006}$ using biased D-log Padé approximants, compared to the exact conjecture of 0.953 125. Later, Lookman and De'Bell [18], using an extended series, estimated $\gamma_1^{(o)} = 0.9549^{+0.0011}_{-0.0015}$ using Baker–Hunter confluent singularity analysis. On the square lattice, using 21 and 23 terms, respectively, Guttmann and Torrie [17] and Cardy and Redner [13] found $\gamma_1^{(o)} = 0.953(6)$ and 0.955(3), using Padé approximants and square-root ratio analysis techniques. Later De'Bell *et al* [15] found $\gamma_1^{(o)} = 0.9541(1)$ using Neville tables, $\gamma_1^{(o)} = 0.9568(8)$ using D-log Padé analysis, and $\gamma_1^{(o)} = 0.951(6)$ using Baker–Hunter analysis. Meirovitch and Chang [10], using Monte Carlo techniques on the square lattice estimated most recently $\gamma_1^{(o)} = 0.9551(3)$.

By setting the interaction parameters, κ_l and κ_r in the partition function to $\kappa_l = 1$ and $\kappa_r = 1$, we can retrieve an 'ordinary' surface, and hence calculate $\gamma_1^{(o)}$. To save space we do not reproduce the tables of the intermediate results. However, the final results are

$$x_c = 0.541\,197 \pm 0.000\,027 \qquad \text{(unbiased second order)} \tag{16}$$

$$\gamma_1^{(o)} = 0.9523 \pm 0.0039 \qquad \text{(unbiased second order)} \tag{17}$$

$$\gamma_1^{(o)} = 0.9528 \pm 0.0042 \qquad \text{(biased second order).} \tag{18}$$

If we do not 'pool' approximants from different series lengths we obtain

$$\gamma_1^{(o)} = 0.9525 \pm 0.0026 \qquad \text{(unbiased second order)} \tag{19}$$

$$\gamma_1^{(o)} = 0.953\,12 \pm 0.000\,52 \qquad \text{(biased second order).} \tag{20}$$

In any case these results are in excellent agreement with the exact values $\gamma_1^{(o)} = 61/64 = 0.953\,125$ and $x_c = 1/\sqrt{2+\sqrt{2}} = 0.541\,196\,1\ldots$.

4.2. The (S–S) model

Numerical evidence of the proposed value for $\gamma_1^{(s)} = 93/64 = 1.453\,125$ has been a little less successful so far. Nearly all estimates are consistently high. For example, using direct enumeration with simple log–log plots, Foster *et al* [16] found $\gamma_1^{(s)} = 1.460(4)$. Grassberger and Hegger [11] and Meirovitch and Chang [10] used Monte Carlo to find $\gamma_1^{(s)} = 1.46(1)$ and 1.478(20), respectively. On the other hand, Guim and Burkhardt [22] used transfer matrices to find $\gamma_1^{(s)} = 1.454(4)$.

To retrieve the (S–S) model we set the interaction parameters κ_l and κ_r in the partition function to $\kappa_l = 1 + \sqrt{2}$ and $\kappa_r = 1 + \sqrt{2}$, that is, the symmetric critical adsorption point. Our final results are

$$x_c = 0.541\,18 \pm 0.000\,05 \qquad \text{(unbiased second order)} \tag{21}$$

$$\gamma_1^{(s)} = 1.448 \pm 0.006 \qquad \text{(unbiased second order)} \tag{22}$$

$$\gamma_1^{(s)} = 1.450 \pm 0.004 \qquad \text{(biased second order)}. \tag{23}$$

Again, these estimates are in excellent agreement with the exact value of $\gamma_1^{(s)} = 1.453\,125$.

The crossover exponent, ϕ_s, has been more difficult to estimate accurately, with results varying from Grassberger and Hegger's [11] $\phi_s = 0.50(1)$ via Monte Carlo techniques to $\phi_s = 0.562(20)$ as found by Meirovitch and Chang [10], again using Monte Carlo. Kremer [21] used renormalization group methods to estimate $\phi_s = 0.55(15)$. Guim and Burkhardt [23] have used transfer matrix techniques to estimate $\phi_s = 0.500(3)$ (this work in fact pools data from (O–S) conditions as well), and Zhao *et al* [20] found $\phi_s = 0.51(4)$ from direct enumeration using partial-differential approximants. Our results are similarly high, with

$$\phi_s = 0.532 \pm 0.024 \qquad \text{(unbiased second order)} \tag{24}$$

$$\phi_s = 0.520 \pm 0.013 \qquad \text{(biased second order)} \tag{25}$$

and so the predicted $\phi_s = \frac{1}{2}$ is just outside our error range. We shall comment later on a possible reason for the difficulty in estimating ϕ_s.

4.3. The (O–S) model

Our main aim is to test numerically Batchelor and Yung's [8] proposed exact result, $\gamma_1^{(m)} = 85/64$, associated with a boundary which is adsorbing on one side of the origin of the walk and ordinary on the other. We can retrieve the (O–S) model by setting the interaction parameters, κ_l and κ_r to $\kappa_l = 1$ and $\kappa_r = 1 + \sqrt{2}$. However, we have used $\kappa_l = 0$ here as this is still in the region where the left side of the surface is repulsive ('ordinary'), but the series are better behaved than at $\kappa_l = 1$.

Again, we give just the final results

$$x_c = 0.541\,18 \pm 0.000\,31 \qquad \text{(unbiased second order)} \tag{26}$$

$$\gamma_1^{(m)} = 1.326 \pm 0.018 \qquad \text{(unbiased second order)} \tag{27}$$

$$\gamma_1^{(m)} = 1.328 \pm 0.006 \qquad \text{(biased second order)} \tag{28}$$

and again the corresponding non-pooled approximants give the more precise values

$$\gamma_1^{(m)} = 1.3274 \pm 0.0009 \qquad \text{(unbiased second order)} \tag{29}$$

$$\gamma_1^{(m)} = 1.3279 \pm 0.0003 \qquad \text{(biased second order)}. \tag{30}$$

Both sets of values strongly support the proposed value of $\gamma_1^{(m)} = 1.328\,125$.

Guim and Burkhardt [23] have effectively found, using a transfer matrix calculation, that the crossover exponent, $\phi_s^{(m)}$, has the value $\phi_s^{(m)} = 0.500(3)$, by pooling data from mixed and fully adsorbing boundary condition cases. We cannot match this precision, which assumes conformal theory. However, we were able to estimate the crossover exponent directly for this transition as

$$\phi_s^{(m)} = 0.527 \pm 0.032 \qquad \text{(unbiased second order)} \tag{31}$$

$$\phi_s^{(m)} = 0.514 \pm 0.014 \qquad \text{(biased second order)} \tag{32}$$

which just encompasses the predicted $\phi_s = \phi_s^{(m)} = \frac{1}{2}$.

5. The phase diagram

In this section we discuss the phase diagram in the κ_l–κ_r plane for SAW attached to a surface on the square lattice. We show that the free energy exists and that there is a first-order transition along the line $\kappa_l = \kappa_r$ for $\kappa_r \geqslant \kappa_a$. The arguments presented rely on results in [1] which were for the square lattice. However, it is possible to extend them to the honeycomb lattice with some work [31]. Although the numerical values of κ_a and μ_{saw} are different on the square lattice, the phase diagram should have the same generic form (see figure 2).

We begin by considering the set A_{nm}^+ of SAW of length n confined to the upper-half of a lattice. The origin of the SAW is attached to the surface, and has m contacts (vertices) with the surface. Here the partition function is given by

$$Z_n^{A^+}(\kappa) = \sum_m c_n^{A^+}(m)\kappa^m \tag{33}$$

where $c_n^{A^+}(m)$ is the number of walks in the set A_{nm}^+ of length n with m contacts with the surface, and κ is the fugacity of contacts with the surface. Hammersley *et al* [1] showed that the reduced free energy per step

$$f^{A^+}(\kappa) = \lim_{n\to\infty} \frac{1}{n} \ln Z_n^{A^+}(\kappa) \tag{34}$$

exists for all κ.

We next consider the set B_{nm}^+ of SAW of length n confined to the positive quadrant of the lattice, with the origin attached to the left-most site of the surface, and whose final vertex is the right-most point of the walk on the surface, with no other site of the walk being as far or further right than this. Here the partition function is given by

$$Z_n^{B^+}(\kappa) = \sum_m c_n^{B^+}(m)\kappa^m \tag{35}$$

where $c_n^{B^+}(m)$ is the number of walks in the set B_{nm}^+ of length n with m contacts with the surface, and κ is the fugacity of contacts with the surface. Hammersley *et al* [1] showed that the reduced free energy per step

$$f^{B^+}(\kappa) = \lim_{n\to\infty} \frac{1}{n} \ln Z_n^{B^+}(\kappa) \tag{36}$$

exists for all κ, and that *importantly*

$$f^{B^+}(\kappa) = f^{A^+}(\kappa). \tag{37}$$

In our notation it is clear that

$$f^{A^+}(\kappa_r) = f(\kappa_r, \kappa_r) \tag{38}$$

where $f(\kappa_r, \kappa_r)$ is given by equation (4) in section 2 (now defined for the square lattice), since $c_n^{A^+}(\kappa_r) = c_n(\kappa_r, \kappa_r)$. Now, since $c_n^{B^+}(m_r) \leqslant c_n(0, m_r)$, and $c_n(m_l, m_r) \geqslant 0$, we have

$$Z_n^{B^+}(\kappa_r) \leqslant Z_n(0, \kappa_r) \leqslant Z_n(\kappa_l, \kappa_r) \leqslant Z_n(\kappa_r, \kappa_r) \tag{39}$$

for $\kappa_l \leqslant \kappa_r$. Taking logarithms and the limits proves, using the sandwich theorem, that the limit

$$f(\kappa_l, \kappa_r) = \lim_{n\to\infty} \frac{1}{n} \ln Z_n(\kappa_l, \kappa_r) \tag{40}$$

exists and is given by

$$f(\kappa_l, \kappa_r) = f(\kappa_r, \kappa_r) \tag{41}$$

for any $0 \leqslant \kappa_l \leqslant \kappa_r$ and for any $\kappa_r \geqslant 0$. Since $c_n(m_l, m_r) = c_n(m_r, m_l)$ then $f(\kappa_l, \kappa_r) = f(\kappa_r, \kappa_l)$. This leads to

$$f(\kappa_l, \kappa_r) = f(\kappa_l, \kappa_l) \tag{42}$$

for any $0 \leqslant \kappa_r \leqslant \kappa_l$.

Now, assuming a single transition (non-analyticity) at some κ_a in $f(\kappa_r, \kappa_r)$ implies that there are two lines of transitions: $0 \leqslant \kappa_l \leqslant \kappa_a$ with $\kappa_r = \kappa_a$ and $0 \leqslant \kappa_r \leqslant \kappa_a$ with $\kappa_l = \kappa_a$. Moreover, these transitions must uniformly have the same singularity in free energy (because of the results (41) and (42)), and so the same crossover exponent (assuming scaling, that is $2 - \alpha_s = 1/\phi_s$ where α_s is the exponent associated with the free energy).

Finally, we argue that the transition line $\kappa_r = \kappa_l$ is a first-order transition (for $\kappa_r = \kappa_l > \kappa_a$). Consider a path of constant $\kappa_r > \kappa_a$ and the partial derivative $\partial f(x, y)/\partial x$ evaluated at $x = \kappa_l, y = \kappa_r$ along that path. For $\kappa_l < \kappa_r$ the partial derivative $\partial f(x, y)/\partial x = 0$ from result (41). However, for $\kappa_l > \kappa_r$ we have $\partial f(x, y)/\partial x = \mathrm{d}f(x, x)/\mathrm{d}x$ from (42), and so since the limit of $\mathrm{d}f(x, x)/\mathrm{d}x$ (as this is evaluated at $x \to \kappa_r$) is strictly positive (a result that follows from the free energy properties for $\kappa_l = \kappa_r$ [1]—that is, it must be a non-decreasing, continuous and convex function—and the assumption of a single transition), there must be a jump at the point $\kappa_l = \kappa_r$ in the derivative $\partial f(x, y)/\partial x$. This indicates that a first-order transition is taking place there. Physically this says that the density of left contacts per step is zero when the polymer is adsorbed on the right, but non-zero when adsorbed on the left, and since by symmetry non-zero when adsorbed equally on both sides. Hence, there must be a jump across the symmetry line.

Hence, we have shown that on the square lattice the full phase diagram in the κ_l–κ_r plane is as shown in figure 2. There are three separate phases: a desorbed phase (in which the free energy is constant), a phase in which SAW adsorbed on the right-hand side of the surface are favoured, and a phase in which SAW adsorbed on the left-hand side of the surface are favoured. The point P is special, being the intersection of two critical lines and one first-order line. It is also novel in terms of the value of its entropic exponent, γ_1. However, the (thermodynamic limit) critical behaviour displayed on crossing through P from D to AL or AR at a fixed angle, whether or not that path lies along BL or BR, is the same as passing through the lines BL and BR in the same fashion. In other words the thermodynamic critical behaviour at P is similar to that at any point on BR or BL—the difference is only in the 'phases' surrounding such points (there are two for any point on BR or BL but three for P).

The same resultant phase diagram can be found by considering partially-directed walks in the presence of a mixed boundary as shown in figure 5, where we consider the square lattice for simplicity. Partially-directed walks are walks which, when viewed from left to right, are forbidden to have any steps to the left. The walk has one step attached to the

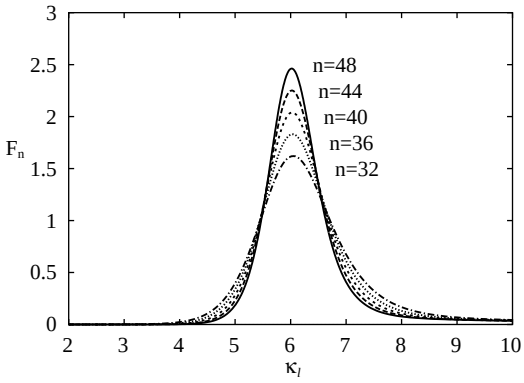

Figure 3. A plot of the fluctuations of the number of left-hand contacts $F_n^l(\kappa_l)$ against κ_l for five values of length ($n = 32, 36, 40, 44, 48$).

surface. As in the full walk problem, any contacts with the right-hand side of the surface are associated with a fugacity κ_r, and contacts with the left-hand side of the surface are associated with a fugacity κ_l (the only difference being that we fix one step along the boundary to make the problem symmetric).

The generating function for all such directed walks is given by essentially the simple product

$$G^{(\text{total})}(x, \kappa_l, \kappa_r) = xG(x, \kappa_l)G(x, \kappa_r) + x \tag{43}$$

where $G(x, \kappa)$ is the generating function of (one-sided) partially-directed walks attached to a surface, since the two legs of the total walk are completely independent of each other (we give the fixed step simply a weight x). The reduced free energy is hence given by

$$f(\kappa_l, \kappa_r) = \max(\ln(x_c^{-1}(\kappa_l)), \ln(x_c^{-1}(\kappa_r))) \tag{44}$$

where $x_c(\kappa)$ is the radius of convergence of the generating function $G(x, \kappa)$ of a partially-directed walk attached to a surface. The phase diagram can then be simply deduced and is the same as for the full undirected problem. So in summary, these partially-directed walks exhibit the same phase diagram as we have argued holds in the case of undirected walks (i.e. walks adsorbed to the left/right of the origin being dominant for $\kappa_l/\kappa_r \geqslant \kappa_a$, and walks to the left and right being equally dominant for $\kappa_l = \kappa_r, \kappa_r \geqslant \kappa_a$).

We have attempted to map out the above transition lines of the full SAW problem on the honeycomb lattice by considering the fluctuations per step of the left- and right-hand contacts with the surface. As described in section 3.2 we plot the fluctuations per step for various fixed κ_r against κ_l and vice versa. The peak in these plots gives an indication of where a transition might be in the κ_l–κ_r plane. The fluctuations of the number of left-hand contacts with the surface per step $F_n^l(\kappa_l, \kappa_r)$ for five lengths is plotted against κ_l for fixed $\kappa_r = 6$ in figure 3. For length 48, we find that this quantity has a maximum at $\kappa_l = 6.019, \kappa_r = 6$, in good agreement with the transition line $\kappa_l = \kappa_r$ for $\kappa_r \geqslant \kappa_a$. We give a final plot of the positions of the peaks in the fluctuations F_n^l and F_n^r per step in figure 4. The positions of the peaks near the symmetry line are fairly constant with changing n and also grow almost linearly in n indicating a δ-function peak (and so a first order transition). The peaks lying along the $\kappa_l =$ constant and $\kappa_r =$ constant sections of the curves are changing position more rapidly with n and are relatively smaller than those associated with the first-order transition; they are also growing more slowly. This is, of course, consistent with the idea that they are

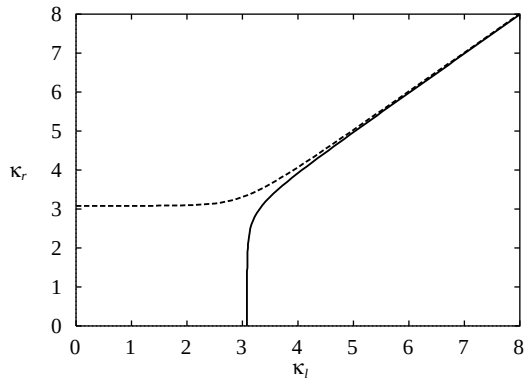

Figure 4. A plot of the positions of the maxima of the fluctuations F_n^l (full curve) and F_n^r (broken curve) for $n = 48$ in the full (κ_l, κ_r) plane.

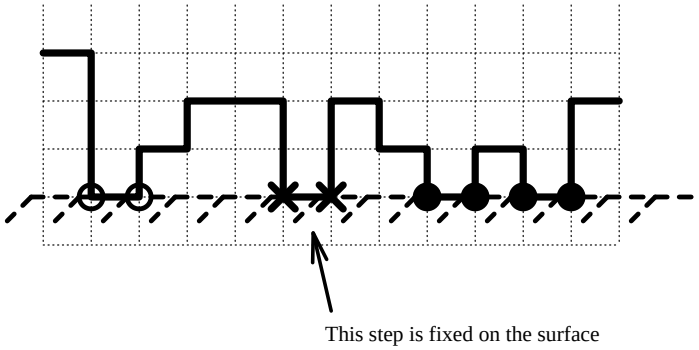

Figure 5. A partially-directed self-avoiding walk on the square lattice with one step attached to a one-dimensional boundary. A fugacity κ_l is associated with contacts on the left-hand side of the surface (open circles), while a fugacity κ_r is associated with contacts on the right-hand side of the surface (closed circles).

associated with a second-order phase transition with $\alpha_s = 0$ ($\phi_s = \frac{1}{2}$). Note that the value $\alpha_s = 0$ implies that the peaks of the fluctuations here should not grow with a power law but may either grow logarithmically or form a jump discontinuity in the thermodynamic limit. Further note that the possibility of logarithms may explain the difficulty in numerically confirming the value $\phi_s = \frac{1}{2}$.

6. Summary

We have considered SAW on the honeycomb lattice in the presence of a mixed boundary; half fixed at the 'ordinary' point and half fixed at the 'special'. For this model we have given numerical support to recent exact results for the critical temperature and configurational exponent, along with a numerical indication that the crossover exponent $\phi_s^{(m)}$ is indeed $\frac{1}{2}$. We have also made similar comparisons for the exponents for SAW with unmixed 'ordinary' and 'special' boundaries.

We find that our results are in good agreement with Batchelor and Yung's [8] claims

that the critical point of the corresponding $O(0)$ model, x_c, is identical for all three cases, and so that the critical point is indeed $1/\sqrt{2+\sqrt{2}}$ with exponent $\gamma_1^{(m)} = 85/64$ for the 'mixed' case. Moreover, we find that the adsorption temperature is given by $\kappa_a = 1+\sqrt{2}$ as they predicted.

We have also elucidated the phase diagram in the κ_l–κ_r plane and found a first-order transition along the line $\kappa_l = \kappa_r$ for $\kappa_r \geqslant \kappa_a$.

Acknowledgments

The authors thank M T Batchelor and C M Yung for sharing their results prior to publication. We are indebted to C Soteros for stimulating discussions and pointing out several crucial references. In addition we thank A J Guttmann, M T Batchelor and C Soteros for carefully reading the manuscript and making several useful suggestions. We are grateful to the Australian Research Council for financial support and DB-W thanks the Graduate School of the University of Melbourne for a scholarship.

References

[1] Hammersley J M, Torrie G M and Whittington S G 1982 *J. Phys. A: Math. Gen.* **15** 539
[2] De'Bell K and Lookman T 1993 *Rev. Mod. Phys.* **65** 87
[3] Cardy J L 1984 *Nucl. Phys.* B **240** 514
[4] Duplantier B and Saleur H 1986 *Phys. Rev. Lett.* **57** 3179
[5] Burkhardt T W, Eisenriegler E and Guim I 1989 *Nucl. Phys.* B **316** 559
[6] Burkhardt T W and Eisenriegler E 1994 *Nucl. Phys.* B **424** 487
[7] Batchelor M T and Yung C M 1995 *Phys. Rev. Lett.* **74** 2026 (1995)
[8] Batchelor M T and Yung C M 1995 *J. Phys. A: Math. Gen.* **28** L421
[9] Batchelor M T and Suzuki J 1993 *J. Phys. A: Math. Gen.* **26** L729
[10] Meirovitch H and Chang I S 1993 *Phys. Rev.* E **48** 1960
[11] Grassberger P and Hegger R 1995 *Phys. Rev.* E **51** 2674
[12] Barber M N, Guttmann A J, Middlemiss K M, Torrie G M and Whittington S G 1978 *J. Phys. A: Math. Gen.* **11** 1833
[13] Cardy J L and Redner S 1984 *J. Phys. A: Math. Gen.* **17** L933
[14] De'Bell K and Essam J W 1980 *J. Phys. C: Solid State Phys.* **13** 481
[15] De'Bell K, Lookman T and Whittington S G 1990 *Phys. Rev.* A **41** 682
[16] Foster D P, Orlandini E and Tesi M C 1992 *J. Phys. A: Math. Gen.* **25** L1211
[17] Guttmann A J and Torrie G M 1984 *J. Phys. A: Math. Gen.* **17** 3539
[18] Lookman T and De'Bell K 1987 *J. Phys. A: Math. Gen.* **20** 763
[19] Whittington S G, Torrie G M and Guttmann A J 1980 *J. Phys. A: Math. Gen.* **13** 789
[20] Zhao D, Lookman T and De'Bell K 1990 *Phys. Rev.* A **42** 4591
[21] Kremer K 1983 *J. Phys. A: Math. Gen.* **16** 4333
[22] Guim I and Burkhardt T W 1989 *J. Phys. A: Math. Gen.* **22** 1131
[23] Guim I and Burkhardt T W 1994 *Phys. Rev.* E **49** 1495
[24] Domany E, Mukamel D, Nienhuis B and Schwimmer A 1981 *Nucl. Phys.* B **190** 279
[25] de Gennes P G 1979 *Scaling Concepts in Polymer Physics* (Ithaca, NY: Cornell University Press)
[26] Nienhuis B 1982 *Phys. Rev. Lett.* **49** 1062
[27] Cardy J L 1989 *Nucl. Phys.* B **324** 581
[28] Burkhardt T W and Xue T 1991 *Nucl. Phys.* B **354** 653
[29] Grassberger P 1982 *Z. Phys.* B **48** 255
[30] Guttmann A J 1989 *Phase Transitions and Critical Phenomena* vol 13, ed C Domb and J L Lebowitz (New York: Academic)
[31] Bennett-Wood D 1996 *PhD Thesis* The University of Melbourne, in preparation